

11p.

# ADVANCES IN X-RAY ANALYSIS

292

Volume 7

N64-31004

Edited by

Code None

Cat-18

*William M. Mueller, Gavin Mallett, and Marie Fay*

**Proceedings of the Twelfth Annual Conference on  
Applications of X-Ray Analysis  
Held August 7-9, 1963**

*Sponsored by*  
University of Denver  
Denver Research Institute

## **AN EXPLANATION OF MICROSTRUCTURES IN THE TANTALUM-CARBON SYSTEM**

G. Santoro and H. B. Probst

*Lewis Research Center  
National Aeronautics and Space Administration  
Cleveland, Ohio*



*Distributed by*  
Plenum Press, New York

# AN EXPLANATION OF MICROSTRUCTURES IN THE TANTALUM-CARBON SYSTEM

G. Santoro and H. B. Probst

*Lewis Research Center  
National Aeronautics and Space Administration  
Cleveland, Ohio*

## ABSTRACT

Compositions in the tantalum-carbon system were prepared by carburizing high-purity tantalum wires. The microstructures so produced exhibit regions of a characteristic striated structure identical to those observed by earlier investigators. There are disparities in the literature as to the origin of such structures in the tantalum-carbon system. They have been variously described as "twins," "striated structure," "precipitate," and "structure of unknown origin." This paper presents conclusive evidence that the structures in question are the result of precipitation on cooling. In addition, a coherent precipitation model is applied in which it is shown that the lattice relationship  $\{0001\}_{\text{Ta}_2\text{C}} \parallel \{111\}_{\text{TaC}}$  can exist with less than 0.5% misfit. This relationship is shown to completely explain the occurrence and characteristic appearance of the observed microstructures. Correlations between chemical analysis, X-ray diffraction results, metallography and microhardness measurements confirm the proposed precipitation model.

31004  
~~2-2-60~~

## INTRODUCTION

Considerable interest has developed in recent years in the tantalum-carbon system. This interest stems primarily from the melting temperatures reported for the compound TaC. This carbide melts at temperatures as high as 3800 to 3900°C<sup>1-3</sup> and is, therefore, one of the highest melting materials known.

Ellinger<sup>4</sup> published the results of his work on the Ta-C system in 1943. His phase diagram showed two carbides, Ta<sub>2</sub>C, a hexagonal structure, and TaC, a NaCl structure. After carburizing a tantalum rod, Ellinger observed a microstructure showing a very definite carbon gradient with concentric bands, which contained two phases, in which the second (minor) phase always existed as apparently straight platelets. Rhines, in the discussion to Ellinger's paper, correctly pointed out that these two-phase regions in binary diffusion couples were simply the result of precipitation occurring on cooling as a result of solubility limits decreasing with temperature.

Since Ellinger's paper, details of the phase diagram have been refined, but the basic qualitative equilibrium relationships are unchanged. An accepted diagram compiled from the results of many investigations is shown in Figure 1.<sup>5</sup> More recently, studies in the Ta-C system<sup>6-9</sup> have revealed microstructures similar to those of Ellinger, but, in many cases, the possibility of these structures being the result of precipitation seems to have been ignored. The characteristic straight platelet structures have been variously described as "twins," "striated structure," and "structure of unknown origin."

<sup>1</sup> References are at the end of the paper.

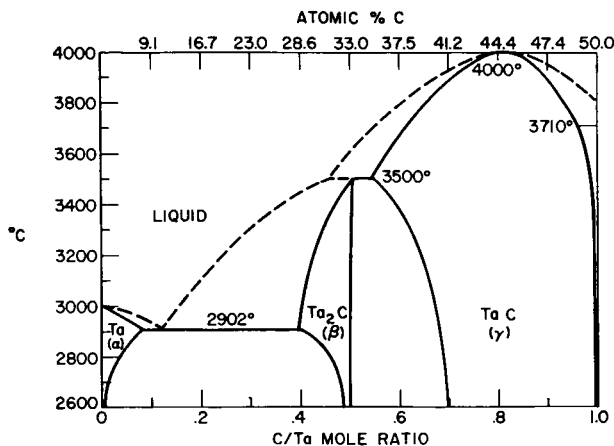


Figure 1. Phase diagram of the Ta-TaC system.<sup>5</sup>

It is the purpose of this paper to show these structures to be the result of precipitation processes and to account for their characteristic appearance by precipitation model based on the geometries of the crystal structures involved.

### EXPERIMENTAL PROCEDURE

The Ta-C compositions for this study were made by carburizing 0.010-in. high-purity tantalum wires in a purified hydrocarbon gas (toluene or propane). The tantalum wire was heated by its own electrical resistance, and the overall carbon content of the resulting structure was controlled by hydrocarbon gas pressure. A detailed account of this method is given by Santoro.<sup>9</sup> The structures studied were produced by heating for 6 hr at 1800°C followed by rapid cooling, unless otherwise specified. Carburized filaments were homogeneous in cross section only if their carbon content placed them well into a single-phase field. Filaments whose overall carbon contents were near the solubility limits of single phases or within a two-phase field were heterogeneous with strongly developed annular structures, i.e., concentric rings. The carbon content reported for any one filament exhibiting an annular structure is an overall composition, and it should be remembered that the case will be of higher carbon content while the core will be lower than the average carbon concentration. The average carbon concentrations were determined by a combustion method and refer to total carbon. The small quantity of sample precluded reliable free-carbon analysis. It is believed, however, that the amount of free carbon is negligible, since no evidence of free carbon was found in the metallographic examinations or the X-ray patterns.

Phase identification was accomplished by standard X-ray diffraction techniques. Diffraction patterns were obtained from as-reacted filament surfaces, powdered filaments, and remaining ductile (unpowderable) cores when these were present. In this manner, phase identification by diffraction was correlated to microstructure.

Metallographic sections of the filaments were prepared by standard mounting and polishing techniques. After investigating several etches, we found that one consisting of HNO<sub>3</sub>/HF in the ratio 3/1 gave the most consistent results. This etch was used for all samples of this study.

Microhardness measurements were made with a  $135^\circ$  diamond pyramid and a 50-g load. This load was determined as the best to give good readings over the wide range of hardnesses from TaC to soft tantalum.

### MODEL

Before examining the actual structures obtained, let us consider a model of precipitation based upon the crystallographic structures involved. Consider the precipitation of  $\beta$  from  $\gamma$  as the solubility limit for tantalum is exceeded during cooling. The matrix  $\gamma$  is a NaCl structure with a lattice parameter, at the solubility limit, of  $4.4104 \text{ \AA}$ .<sup>10</sup> The arrangement of a unit cell of this structure is shown in Figure 2 (not taking into account vacant carbon sites). Any  $\{111\}$  plane of this structure may be considered to consist entirely of carbon or tantalum atoms in a hexagonal arrangement with a spacing of  $3.12 \text{ \AA}$  between nearest neighbors.

The  $\beta$  phase, which must precipitate from  $\gamma$ , has a hexagonal structure and must be saturated in carbon. The lattice parameters for the  $\beta$  phase are  $a_0 = 3.104 \text{ \AA}$  and  $c_0 = 4.942 \text{ \AA}$ ; a unit cell is shown in Figure 3. The basal plane of this structure consists of a hexagonal arrangement of tantalum (or carbon) atoms with a nearest-neighbor spacing of  $3.104 \text{ \AA}$ .

Comparison of the  $\{111\}$  plane of  $\gamma$  and the basal plane of  $\beta$  shows that both have identical geometries with a linear mismatch of only about 0.5%; thus a very favorable situation exists for  $\beta$  to precipitate on  $\{111\}$  planes of  $\gamma$  on cooling. The same geometrical situation exists if  $\gamma$  precipitates from  $\beta$ . The same compositions and therefore lattice parameters must be considered, and it is therefore seen that  $\gamma$  precipitation on the basal plane of  $\beta$  is also highly probable.

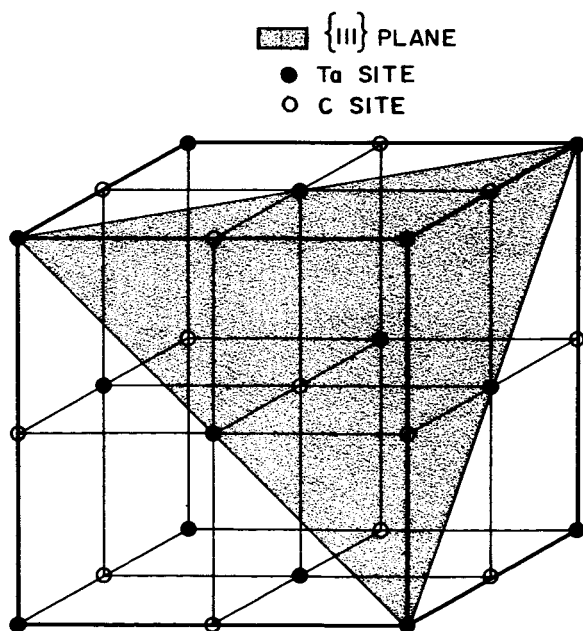


Figure 2.  $\gamma$ (TaC) Unit Cell.

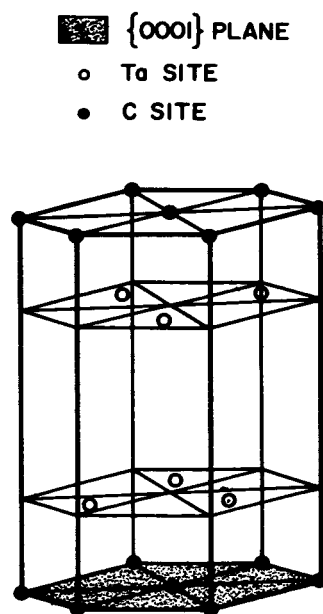


Figure 3.  $\beta$  ( $\text{Ta}_2\text{C}$ ) Unit Cell.

Precipitation reactions with such lattice relationships have been observed in metal systems. For example, hexagonal  $\text{AgAl}_2$  precipitates from silver-saturated face-centered cubic aluminum solid solution so that the  $\{0001\}$  plane of  $\text{AgAl}_2$  is parallel to the  $\{111\}$  plane of the aluminum solution.<sup>11</sup> An example of a cubic precipitate from a hexagonal matrix is found in the manganese-tin system.<sup>12</sup> In this case the simple cubic ( $\text{CaF}_2$  structure)  $\text{Mg}_2\text{Sn}$  precipitates with its  $\{111\}$  plane parallel to the  $\{0001\}$  plane of the magnesium solid-solution matrix. Although the habit plane and direction in the  $\text{Mg}_2\text{Sn}$  precipitate can be varied by heat treatment, the precipitate is always rejected from solution on the basal plane of the matrix.

In the case of  $\text{TaC-Ta}_2\text{C}$  precipitation, it is not assumed here that there is necessarily a coherency between matrix and precipitate, but only that the plane of the matrix on which precipitation occurs is the close-packed plane (i.e.,  $\{111\}$  for the cubic  $\text{TaC}$  matrix and  $\{0001\}$  for the hexagonal  $\text{Ta}_2\text{C}$  matrix). The high degree of matching between these planes does suggest, however, that coherent precipitation is a very distinct possibility.

If the close-packed planes are the precipitation planes as assumed here, then the precipitation of either carbide from the other should result in a Widmanstätten structure—there should be characteristic differences, however, depending on which carbide is the matrix. In the precipitation of  $\beta$  from  $\gamma$ , the  $\{111\}$  plane of  $\gamma$  actually provides four potential precipitation planes, since in the cubic geometry there are four  $\{111\}$  planes. Therefore in a single grain of  $\gamma$ , platelets of  $\beta$  precipitate might be expected in up to four directions. Conversely, when  $\gamma$  precipitates from  $\beta$ , the singular basal plane of the hexagonal symmetry provides but one precipitation plane. Hence, in a single grain of  $\beta$  the platelets of  $\gamma$  precipitate should be found in only one direction.

## EXPERIMENTAL RESULTS

Numerous microstructures in the  $\text{Ta-C}$  system were examined. Representative structures will be discussed here proceeding from high-carbon to low-carbon compositions.

### $\text{TaC}_{0.88}$

Figure 4 shows the structure corresponding to a composition of  $\text{TaC}_{0.88}$  well within the  $\gamma$  single-phase field. The structure shows a single-phase material and is representative of all compositions between  $\text{TaC}_{0.74}$  and  $\text{TaC}_{0.98}$ . X-ray analysis of such a structure gives only the  $\text{TaC}$  pattern, and the hardness of this particular composition is DPH 2700.

### $\text{TaC}_{0.64}$

The structure obtained at a composition of  $\text{TaC}_{0.64}$  is shown in Figure 5. The characteristic annular structure is apparent. X-ray analysis of this material shows the presence of both  $\gamma$  and  $\beta$ .<sup>\*</sup> Such a two-phase structure is characteristic of compositions between  $\text{TaC}_{0.52}$  and  $\text{TaC}_{0.74}$ . Slow cooling of samples within this composition range gave identical structures, thus ruling out the possibility of these structures being the result of metastable transformations. Within this range, as lower carbon concentrations are approached, the  $\beta$  phase becomes more evident in the X-ray patterns, the inner structure (core) occupies a larger portion of the cross section, and a small central core of single-phase  $\beta$  becomes evident. The hardness of the two zones shown in Figure 5 are

<sup>\*</sup> Some lines corresponding to those reported by Lesser and Brauer<sup>13</sup> as belonging to an unknown zeta phase were observed for some compositions between  $\text{TaC}_{0.4}$  and  $\text{TaC}_{0.6}$ . The origin and significance of this phase is not known at the present time.

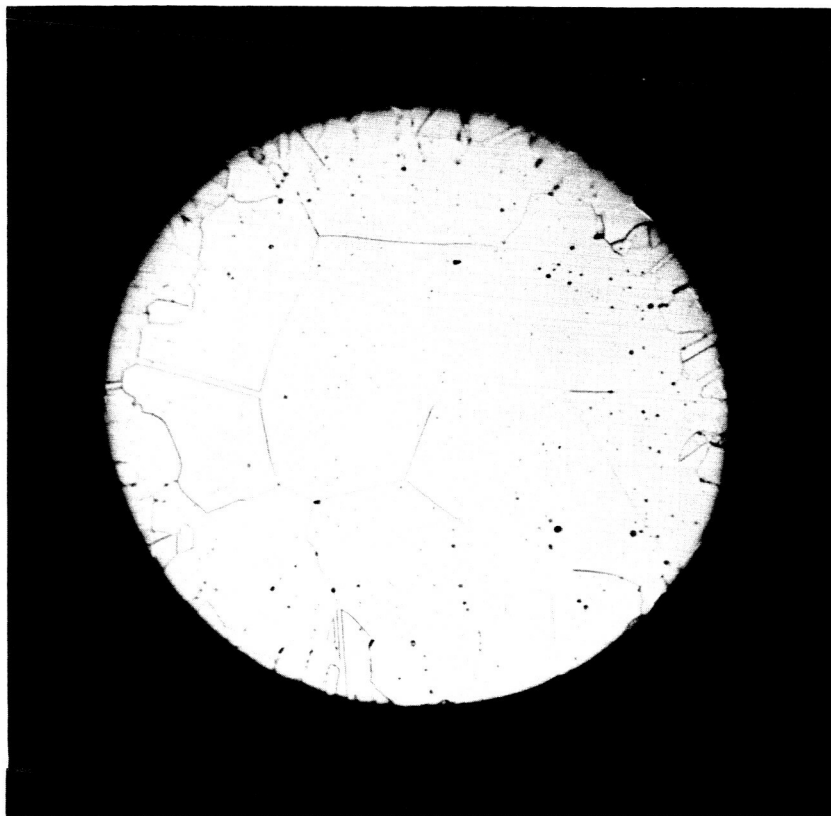


Figure 4. Microstructure of TaC<sub>0.88</sub>; etchant, 3HNO<sub>3</sub>/HF; 300 $\times$ ; DPH = 2700.

DPH 1620 and DPH 1520 for the case and core, respectively. This hardness for the core represents an increase over that of single-phase  $\beta$  (DPH  $\approx$  1000), while the value for the case seems to be essentially the same as carbon-deficient  $\gamma$  (DPH  $\approx$  1600).<sup>9</sup>

The appearance of this structure and the results of X-ray diffraction ( $\gamma$  and  $\beta$  present) give support to the proposed precipitation model. During the carburizing treatment, a carbon-deficient  $\gamma$  of the case was in equilibrium with the carbon-saturated  $\beta$  core. Upon cooling solubility limits were exceeded with  $\beta$  precipitating from  $\gamma$  in the case and  $\gamma$  precipitating from  $\beta$  in the core according to the proposed lattice relationship. The multidirectional platelets of  $\beta$  are evident in the case, while the core exhibits unidirectional  $\gamma$  platelets within any one  $\beta$  grain. The increasing size of the core with decreasing carbon and the eventual stabilization of a small single-phase  $\beta$  core are in accord with the equilibrium diagram shown in Figure 1 and with the proposed explanation of the microstructures. Another observation in support of the precipitation model is the fact that in all carburized samples exhibiting both unidirectional and multidirectional structures the region containing the multidirectional platelets is always located nearer the sample surface than the unidirectional structure. This is in accord with the carbon gradient that exists at the carburizing temperature, i.e., the  $\gamma$  phase from which  $\beta$  precipitates, being

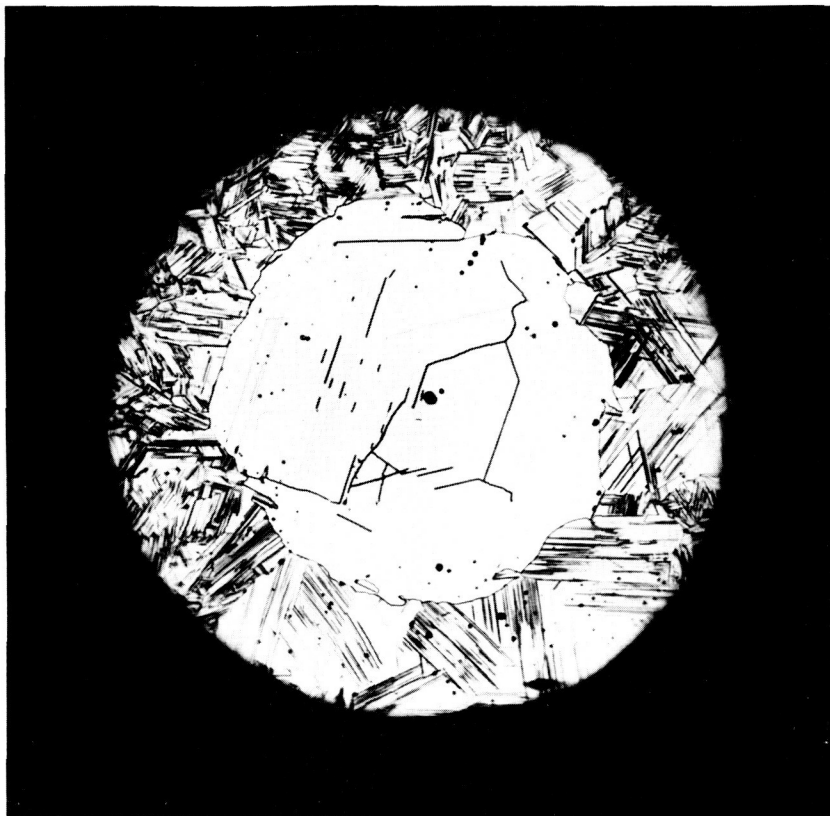


Figure 5. Microstructure of TaC<sub>0.64</sub>; etchant, 3HNO<sub>3</sub>/HF; 300 ×; DPH case = 1620, DPH core = 1520.

of higher carbon content, is located nearer the surface than the  $\beta$  from which  $\gamma$  precipitates; thus the  $\gamma$  matrix with multidirectional  $\beta$  precipitate is always found nearer the sample surface than the lower-carbon  $\beta$  matrix containing unidirectional  $\gamma$  precipitate.

The constant solubility of carbon in  $\beta$  as a function of temperature as indicated in Figure 1 must be in error, since the observed precipitation of  $\gamma$  from  $\beta$  is indicative of decreasing carbon solubility in  $\beta$  with decreasing temperature. Similar structures have been found in work with the niobium-carbon system; however, no such structures were observed in the hafnium-carbon system.<sup>7</sup> This again supports the precipitation explanation proposed here, since these observations are obviously due to the similarity between the tantalum-carbon and niobium-carbon equilibrium relationships (both exhibiting a dimetal carbide), while in the hafnium-carbon system an equilibrium dimetal carbide does not exist.

The hardness values for the structures shown in Figure 5 suggest that the presence of a hard  $\gamma$  precipitate in a relatively soft  $\beta$  matrix (the core) increases the hardness over that of the  $\beta$  matrix (DPH = 1000) while, conversely, the presence of  $\beta$  precipitate in the very hard  $\gamma$  matrix shows little effect on the hardness as compared to that on the hardness of single-phase carbon-deficient  $\gamma$  (DPH  $\approx$  1600<sup>9</sup>).

**TaC<sub>0.31</sub>**

A typical structure resulting at low carbon concentrations is shown in Figure 6. At the composition of TaC<sub>0.31</sub>, Figure 1 shows the equilibrium phases to be  $\alpha$  and  $\beta$ .<sup>\*</sup> X-ray analysis of the surface of the as-reacted sample gave only the  $\beta$  pattern, while analysis of the core alone (after removing the brittle case) gave both  $\beta$  and  $\alpha$ . The hardness of the case is DPH 860 possibly representing a slight decrease of hardness for carbon-deficient  $\beta$  as compared to DPH 1000 for carbon-saturated  $\beta$ . This is in agreement with Samsonov,<sup>14</sup> who gives hardness values of 810 and 947 for carbon-deficient and carbon-saturated  $\beta$ , respectively. The core has a hardness of DPH 120, and this, along with X-ray results and appearance, suggests a random precipitation of  $\beta$  in  $\alpha$ . Structures similar to that of Figure 6 were obtained at all compositions below about TaC<sub>0.43</sub> with the  $\alpha$  matrix core occupying a larger portion of the cross section as the carbon concentration is decreased. At compositions above TaC<sub>0.43</sub>, near  $\beta$ , the entire cross section appeared as the case in Figure 6. While X-ray analysis showed only  $\beta$  for such structures, the dark, apparently lamellar, regions appear to be a second phase and warranted further investigation.

\* Samples consisting of only single-phase  $\beta$  are difficult to make by the carburization method owing to the limited composition range of the phase at low temperatures.

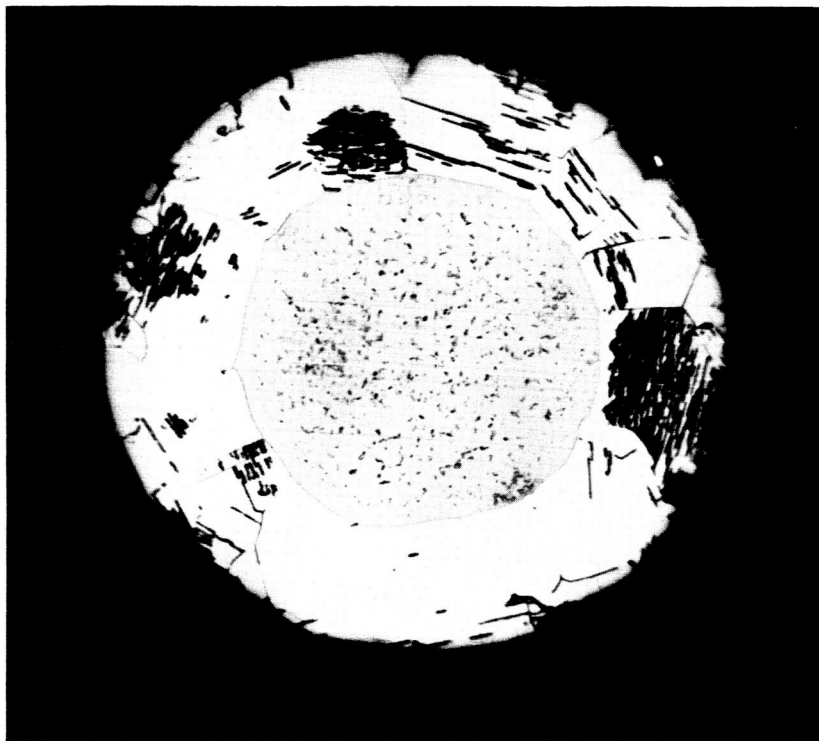


Figure 6. Microstructure of TaC<sub>0.31</sub>; etchant, 3HNO<sub>3</sub>/HF; 300 $\times$ ; DPH case = 860, DPH core = 120.



This lamellar structure is of particular interest, since Ellinger<sup>4</sup> observed similar but somewhat better-developed structures in his low-carbon sample and Rhines in the discussion of Ellinger's paper suggested these might be the result of a low-temperature eutectoid decomposition of  $\beta$  to  $\alpha + \gamma$ . With this in mind, a sample was prepared at a composition of  $\text{TaC}_{0.36}$  and slowly cooled from the reaction temperature (a period of  $1\frac{1}{4}$  hr to cool to  $\approx 800^\circ\text{C}$ ) in order to allow full development of a eutectoid structure if it exists. The resulting structure is shown in Figure 7. A lamellar structure in the case (which was  $\beta$  at the reaction temperature) was indeed developed; however, X-ray patterns from the surface of this sample showed the presence of  $\alpha + \beta$  and not  $\alpha + \gamma$ . This then indicates that eutectoid decomposition of  $\beta$  does not occur; however, a lamellar structure was developed by this treatment and must be explained. Since the two phases present as indicated by X-ray are  $\beta$  and  $\alpha$ , it would appear that this structure represents a precipitate of  $\alpha$  in a  $\beta$  matrix. The difference between this well-developed lamellar structure and that of Figure 6 must be due to a slow cooling rate, which leads to a more complete precipitation and the elimination of nonequilibrium supersaturated solid solution that results by quenching.

The hardness of the two-phase  $\alpha + \beta$  case is 770, while that of the core is 120. These compare well with the hardnesses of the rapidly cooled structure of Figure 6, showing a slight decrease in the hardness of the case due to the presence of the soft  $\alpha$  precipitate.



Figure 7. Microstructure of  $\text{TaC}_{0.36}$ ; slow cool—etchant,  $3\text{HNO}_3/\text{HF}$ ;  $300\times$ ; DPH case = 770, DPH core = 120.

The unidirectional nature of the  $\alpha$  precipitate in  $\beta$  is interesting. Comparison of the two close-packed planes of the two phases shows the {110} plane of carbon-saturated  $\alpha$  to be a distorted hexagonal arrangement with nearest-neighbor spacings of 2.865 and 3.305 Å and included angles within the unit triangle to be 54.7, 54.7, and 70.6°—calculated from  $a_0 = 3.305$  Å for tantalum.<sup>13</sup> This compares to the true hexagonal arrangement in the {0001} plane of tantalum saturated  $\beta$  in which the nearest-neighbor spacing is 3.101 Å and of course the included angles are all 60°. This comparison yields an average mismatch of about 2.7% for placing one unit triangle upon the other; however, this misfit increases as the precipitate grows.

The fact that  $\alpha$  seems to precipitate from  $\beta$  in a Widmanstätten structure while the  $\beta$  precipitation from  $\alpha$  appears to be the random (see the core of Figure 6) may be due to the increasing misfit with size of precipitate. In the case where lamellar structures form, the metallic bonding of the  $\alpha$  phase may allow it to readily distort to accommodate the increasing misfit and thus grow as a continuous platelet. On the other hand, the hybrid metallic-covalent bonding of the  $\beta$  phase does not allow such distortion; thus as the  $\beta$  precipitate grows, it may lose coherency with the  $\alpha$  matrix and random precipitation may result.

## CONCLUSIONS

As a result of this investigation, the following conclusions may be drawn:

1. The characteristic striated (Widmanstätten) structures found in the tantalum-carbon system at compositions between  $Ta_2C$  and  $TaC$  are the result of precipitation reactions in which the close-packed plane of each phase is the plane of precipitation.
2. The maximum solubility of carbon in  $Ta_2C$  must decrease with decreasing temperature rather than remain constant as the presently accepted phase diagram indicates.
3. There is no evidence for a eutectoid decomposition of  $Ta_2C$ .
4. Tantalum can precipitate from  $Ta_2C$  giving a unidirectional Widmanstätten structure; however,  $Ta_2C$  precipitation from tantalum is random apparently because of the inability of  $Ta_2C$  to distort in order to maintain coherency with the tantalum matrix.

## REFERENCES

1. E. Friederich and L. Sittig, *Z. anorg. u. Allgem. Chem.* **144**: 174, 1925.
2. C. Agte and H. Alterthum, *Z. tech. Physik.* **11**: 182, 1930.
3. C. F. Zalabak, NASA TN D-761, March, 1961.
4. F. H. Ellinger, *Trans. ASM* **31**: 89, 1943.
5. E. K. Storms, LAMS-2674, Pt. 1, February 1, 1962.
6. R. T. Dolloff, Progress Report No. 1, National Carbon Co., Contract AF 33(657)-8025, June 10, 1962.
7. High-Temperature Materials, Inc., Final Report, Contract NOW60-0292, September 30, 1961.
8. E. J. Vargo, Thompson Ramo Wooldridge, Inc., TM-1575-CM, June 29, 1960.
9. G. Santoro, *Trans. AIME* **227**: 1361, 1963.
10. A. L. Bowman, *J. Phys. Chem.* **65**: 1596, 1961.
11. R. F. Mehl and C. S. Barrett, *Trans. AIME* **93**: 78, 1931.
12. G. Derge, A. R. Kommel, and R. F. Mehl, *Trans. AIME* **124**: 367, 1937.
13. R. Lesser and G. Brauer, *Z. Metallk.* **49**: 622, 1958.
14. G. V. Samsonov and V. B. Rukina, *Dopovidi Akad. Nauk Ukr. RSR* No. 3: 247, 1957.

## DISCUSSION

*G. F. Carter* (E. I. du Pont de Nemours and Co.): The phase rule says that if you have only a two-component system you cannot form a two-phase diffusion zone. Would that be in complete agreement with your observations of the two-phase zone being a result of precipitation?

*H. B. Probst*: Yes.

*G. F. Carter*: At the temperature of your diffusion experiment you could form only three phases. Assume that the core would be  $\alpha$ , and surrounding that would be  $\beta$  and surrounding that would be  $\gamma$ . Of course, as you diffused more and more carbon into that you would convert  $\alpha$  to  $\beta$  and  $\beta$  to  $\gamma$  and so on.

*H. B. Probst*: That is correct. To clarify this point, let's consider a diffusion treatment carried out for sufficient time to eliminate the low-carbon  $\alpha$  region so that at the diffusion treatment temperature there exists a single-phase  $\beta$  core and a single-phase  $\gamma$  case in accord with the phase rule; that is, only single-phase regions are present. Now, referring to the phase diagram, at the interface between case and core the  $\gamma$  phase is saturated with respect to tantalum, and its composition at the interface is that indicated by the phase diagram as the point on the curve separating the  $\gamma$  field from the  $\beta + \gamma$  field at the diffusion temperature. Likewise, the  $\beta$  core at the interface is saturated with respect to carbon, and its composition at the interface is the point on the curve separating the  $\beta$  field from the  $\beta + \gamma$  field at the diffusion temperature. Upon cooling, these compositions pass into the two-phase field  $\beta + \gamma$ , and consequently  $\beta$  precipitates from  $\gamma$  and  $\gamma$  precipitates from  $\beta$ , resulting in the two-phase regions observed in the microstructures. This precipitation continues to occur on cooling as compositions away from the interface reach their solubility limits at lower temperatures. The distance from the interface that precipitation might be observed is dependent on two unknown factors. They are the compositional gradients present at the diffusion temperature and the shape of solubility-limit curves in the phase diagram down to room temperature.